BPQP: A Differentiable Convex Optimization Framework for Efficient End-to-End Learning

Jianming Pan
Haas School of Business
University of California, Berkeley
Berkeley, CA 430072
jianming_pan@berkeley.edu

Xiao Yang
Microsoft Research
Beijing, China
Xiao.Yang@microsoft.com

Jiang Bian
Microsoft Research
Beijing, China
Jiang.Bian@microsoft.com

Abstract

Real-world decision-making processes often employ a two-stage approach, where a machine learning model first predicts key parameters, followed by a constrained convex optimization model to render final decisions. The machine learning model is typically trained separately to minimize prediction error, which may not necessarily align with the ultimate goal, resulting in potentially suboptimal decisions. The predict-then-optimize approach offers an end-to-end learning solution to bridge this gap, wherein machine learning models are trained in tandem with the optimization model to minimize the ultimate decision error. However, practical applications involving large-scale datasets bring about significant challenges due to the inherent need for efficiency to fully realize the potential of the predict-then-optimize approach. Although recent works have started to focus on predict-then-optimize, they have been limited to small-scale datasets due to low efficiency. In this paper, we propose BPQP, a differentiable convex optimization framework for efficient end-to-end learning. To address the challenge of efficiency, we initially reformulate the backward pass as a simplified and decoupled quadratic programming problem by exploiting the structural trait of the KKT matrix, followed by solving it using first-order optimization algorithms. Extensive experiments on both simulated and real-world datasets have been conducted, demonstrating a considerable improvement in terms of efficiency – at least an order of magnitude faster in overall execution time. To the best of our knowledge, our work is the first to apply the predict-then-optimize paradigm to large-scale, real-world scenarios. We address the efficiency issue and highlight the superiority of BPQP over the traditional two-stage learning approach.

1 Introduction

Data-driven stochastic optimization often relies on a two-stage solution: first, it reduces uncertainty by predicting key unknown parameters based on available contextual features, then it utilizes these predictions for downstream constrained optimization. The *predict-then-optimize* paradigm [1–3] integrates these two stages, enabling end-to-end training to directly minimize *regret* – the difference between the decision made from the prediction and the optimal decision in hindsight [4, 5]. This paradigm, and closely related data-driven optimization methods [6–8], have proven effective in

37th Conference on Neural Information Processing Systems (NeurIPS 2023).

various applications, such as portfolio optimization [2], shortest path programming [9], and electric power allocation [10].

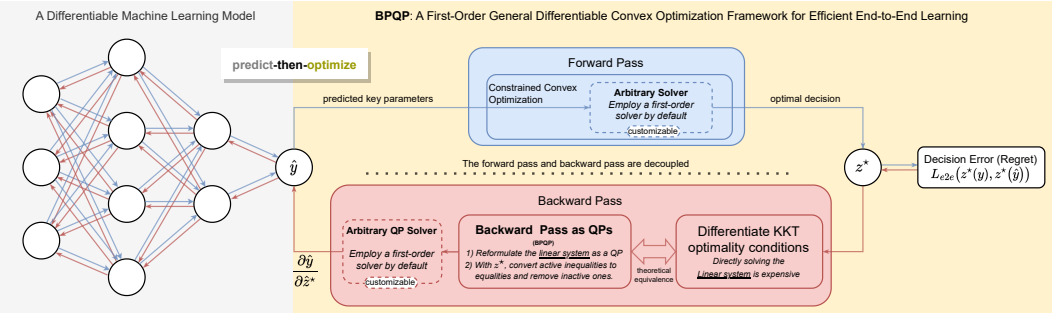

Figure 1: The learning process of BPQP: the machine learning model outputs key parameters $\hat{y}$ and then generates the optimal decision $z^\star$ in the forward pass; the backward pass propagates the decision error to the machine learning model for end-to-end learning; the process is accelerated by reformulating and simplifying the problem first and then adopting efficient solvers.

Training such an end-to-end model necessitates the incorporation of external differentiable layers into the training loop of a machine learning (ML) model. Differentiable convex layers [2, 8, 11] leverage second-order optimization algorithms (e.g., the primal-dual interior point method) in the forward pass to obtain optimal solutions, and then share necessary gradient information in the backward pass to facilitate nearly cost-free backpropagation. However, the drawback of second-order algorithms is their difficulty with warm-starts and their poor scalability for very large problems [12]. For large-scale applications, first-order optimization algorithms are more common [13–15], but they do not readily lend themselves to sharing differential structure information. This limits the choice of optimization algorithms and makes it difficult to achieve overall efficiency. To enable rapid, tractable gradient computation and further expand the capabilities of the predict-then-optimize paradigm, we propose a general, first-order differentiable convex framework for large-scale end-to-end learning, namely BPQP.

Specifically, we solve the forward and backward passes in a "decoupled" manner, which enables the use of any optimization algorithms (with first-order as default) that best match the problem structure and allows for large-scale training. This new framework is realized by reformulating the **B**ackward **P**ass as a **Q**uadratic **P**rogramming (BPQP) problem that relies solely on the Karush-Kuhn-Tucker (KKT) matrix, and using the first-order Alternating Direction Method of Multipliers (ADMM) [12] to track accurate gradients. Since there is no need for structured information sharing in the forward pass, the computational time for the entire predict-then-optimize process can be significantly reduced. This key idea is summarized in Fig. 1.

Our proposed framework has several theoretical and practical contributions:

Efficient Gradients Computation: Empirically, BPQP significantly improves the overall computational time, achieving up to $21.17\times$, $16.17\times$, and $1.67\times$ faster performance over existing differentiable layers on 100-dimension Linear Programming, Quadratic Programming, and Second Order Cone Programming, respectively. Furthermore, when applied to large-scale real-world portfolio optimization, BPQP enhances the Sharpe ratio from 0.65(±0.25) to 1.28(±0.43) compared to widely-adopted methods designed for the two-stage approach.

Flexible Solver Choice: BPQP accommodates any general-purpose convex solver to integrate the differentiable layer for end-to-end training. In addition, we propose a specialized method for the backward pass: Backward Pass as Quadratic Programming (BPQP). This method leverages structural traits such as sparsity, solution polishing [12], and active-sets [16] for efficient and accurate gradients computation. The method uses Quadratic Programming (QP) to avoid the inversion of the KKT matrix and enables *large-scale gradients computation* via the Alternating Direction Method of Multipliers (ADMM). This flexibility in solver choice allows for better matching of solver capabilities with specific problem structures, potentially leading to improved efficiency and performance.

2 Related works

Differentiable convex layer For a convex optimization model, the KKT conditions are first-order necessary conditions for a solution to be optimal. The gradients can be generated by applying the Implicit Function Theorem to KKT conditions. Based on the above design, some approaches have demonstrated success in creating a differentiable convex layer without compromising accuracy. OptNet [8] presented a differentiable batched-GPU QP solver. [10] proposed a predict-and-optimize model within the context of stochastic programming. diffcp [7, 6] considers computing the derivative of convex cone program by implicitly differentiating the residual map for its homogeneous self-dual embedding. Open-source convex solver CVXPY [17] adopts a similar method and computes gradients by SCS [18]. In this work, we mainly compare BPQP to OptNet and CVXPY.

Learn-to-optimize As a comparison to compute for exact gradients, existing work on *Learn-to-Optimize* trains an approximated solver network via SGD (e.g. DC3 [19]) or RL policy gradients [20–23] to solve constrained optimization problems that have a true graphical structure e.g. TSP, VRP, Minimum Vertex Cover, Max-Cut, and their variants. Leveraging the strong representation ability of state-of-the-art graph-based networks, RL obtains final solutions or intermediate results to be polished by searching or optimization algorithms. When optimizing convex and hard constraints in real-world scenarios, the underlying graph is typically fully connected and the accuracy tolerance is lower[24]. This presents a restriction on the widely usage of works based on approximated solvers.

3 Background

3.1 Predict-then-optimize Framework

In this section, we formally describe the predict-then-optimize framework for stochastic decision making problems. We assume that the problem of our interest has convex objective and constraints, but the key parameter $y \in \mathbb{R}^p$ is not observable when the decision is made. For each optimization instance, a prediction of y is required to solve the downstream deterministic optimization problem. Specifically, let $(x \in \mathcal{X}, y \in \mathcal{Y}) \sim \mathcal{D}$ denote standard input-output pairs drawn from the real and unknown distribution $\mathcal{D}$. Suppose a ML model $\mathcal{N}$, parameterized by θ, with input features x is trained to generate such prediction $\hat{y} = \mathcal{N}(x;\theta) = \mathbb{E}_{y\sim p_\theta(y|x)}[y]$, namely $\hat{y} \in \mathbb{R}^p = \mathbb{E}[y|x]$. Let $z_{\hat{y}} \in \mathbb{R}^d$ denote the decision variable of the corresponding optimization relying on random parameter $\hat{y}$. The parameterized convex optimization can be formalized as follows:

$$z^\star_{\hat{y}} = \underset{z\in\mathbb{R}^d}{\arg\min}\ f_{\hat{y}}(z) \quad \text{subject to } \ h_{\hat{y}}(z) = 0,\ g_{\hat{y}}(z) \leq 0, \tag{1}$$

For any given $\hat{y}$, $f_{\hat{y}}(\cdot) : \mathbb{R}^d \to \mathbb{R}$ the C^2 continuous convex objective function, and $h_{\hat{y}}(\cdot) : \mathbb{R}^d \to \mathbb{R}^n,\ g_{\hat{y}}(\cdot) : \mathbb{R}^d \to \mathbb{R}^m$ the n-dimension equality constraints and m-dimension inequality constraints representing the feasible region. h and g are both C^2 continuous convex functions. As we demonstrated, optimal decision $z^\star$ is a random variable depending on $\hat{y},\ z^\star_{\hat{y}\sim p_\theta(y|x)}$.

To implement an end-to-end approach training for $\mathcal{N}$, upon observing the optimal decision $z^\star_y$ relative to the true instantiation of x and y, we update the parameterized model $\mathcal{N}(x;\theta)$ correspondingly, minimizing regret. The overall end-to-end training procedure can be viewed as maximizing posterior probability given decision error and prediction error.

$$p(\theta|regret, y, x) \propto \underbrace{p(regret|y,x,\theta)}_{\text{Decision Error}}\underbrace{p(y|x,\theta)p(x|\theta)}_{\text{Prediction Error}}\underbrace{p(\theta)}_{\text{prior}}, \tag{2}$$

Ideally, our goal here is to use supervised learning to predict the unspecified parameter $\hat{y}$ from empirical data in ways that the decisions made from estimation $z^\star_{\hat{y}}$ match the best decisions taken in hindsight $z^\star_y$, i.e., regret

$$\text{regret}(y,\hat{y}) = f_y\left(z^\star_{\hat{y}}\right) - f_y\left(z^\star_y\right), \tag{3}$$

Given the realized parameter y, [25] found the exact optimization decision error empirically to be a narrow (Dirac-like) target distribution centered at the ground truth $regret = 0$. The rest of the terms above can be viewed as *prior* distribution forms the classic prediction error of which we

choose simple MSE loss, yielding the simplified end-to-end (predict-then-optimize) loss, weighted by constant $\beta \in (0, 1)$:

$$\mathcal{L}_{e2e} = \beta \underbrace{\mathbb{E}_{x,y\sim\mathcal{D}}\left[\left\|f_y\left(z^\star_{\hat{y}}\right) - f_y\left(z^\star_y\right)\right\|^2\right]}_{\text{Decision Error: } \textit{regret}} + \underbrace{\mathbb{E}_{x,y\sim\mathcal{D}}\left[\|y - \hat{y}\|^2\right]}_{\text{Prediction Error}} + \alpha \underbrace{\mathcal{L}_{reg}(\theta)}_{\text{prior}}. \tag{4}$$

Comparison to Two-stage Approach The two terms in Eq. (4) are concerned with decision error and prediction error. The former is often approximated as surrogate loss due the complexity of computing regret in previous work [1, 2]. But surrogate loss is sub-optimal and often cannot handle learning feasible solutions of complex constraints over thousands or even hundreds of dimensions. Relatively, the traditional Two-stage approach divides stochastic optimization into two separate stages: first train a prediction model on y and then solve the optimization problems $z^\star_{\mathbb{E}[y|x]}$ separately. The shortcoming of the Two-stage approach is that it does not take the effect on the optimization task into account. Training to minimize Two-stage loss (prediction loss) is not guaranteed to deliver better performance in terms of the decision problem [5, 11]. As a special case of end-to-end loss, we conclude that the Two-stage approach minimizes a lower bound of the total end-to-end loss and does not necessarily result in the minimization of regret.

$$\mathcal{L}_{2stage} = \mathbb{E}_{x,y\sim\mathcal{D}}[\|y - \hat{y}\|^2] \leq \mathcal{L}_{e2e}. \tag{5}$$

3.2 Differentiating Through KKT Conditions

One major challenge of adopting predict-then-optimize approach is to backpropagate losses through the argmin operator, namely backward pass.

$$\frac{\partial \mathcal{L}}{\partial y} = \frac{\partial \mathcal{L}}{\partial z^\star}\frac{\partial z^\star}{\partial y}, \tag{6}$$

We consider a general convex problem in Eq. (1). To compute the derivative of the solution $z^\star$ to parameter y, OptNet [8] differentiates the KKT conditions using techniques from matrix differential calculus. Following this method, the Lagrangian is given by (omitting y),

$$L(z, \nu, \lambda) = f(z) + \nu^\top h(z) + \lambda^\top g(z), \tag{7}$$

where $\nu \in \mathbb{R}^m$ and $\lambda \in \mathbb{R}^n$, $\lambda \geq 0$ respectively denotes the dual variables on the equality and inequality constraints. The sufficient and necessary conditions for optimality of Eq. (1) are KKT conditions. Applying the Implicit Function Theorem (IFT) to the KKT conditions and let $P(z^\star, \nu^\star, \lambda^\star) = \nabla^2 f(z^\star) + \nabla^2 h(z^\star)\nu^\star + \nabla^2 g(z^\star)\lambda^\star$, $A(z^\star) = \nabla h(z^\star)$ and $G(z^\star) = \nabla g(z^\star)$. Let $q(z^\star, \nu^\star, \lambda^\star) = \partial(\nabla f(z^\star) + \nabla h(z^\star)\nu^\star + \nabla g(z^\star)\lambda^\star)/\partial y$, $b(z^\star) = \partial h(z^\star)/\partial y$ and $c(z^\star, \lambda^\star) = \partial(D(\lambda^\star)g(z^\star))/\partial y$. Then the matrix form of the linear system can be written as:

$$\begin{bmatrix} P(z^\star, \nu^\star, \lambda^\star) & G(z^\star)^\top & A(z^\star)^\top \\ D\left(\lambda^\star\right) G(z^\star) & D\left(g(x^\star)\right) & 0 \\ A(z^\star) & 0 & 0 \end{bmatrix} \begin{bmatrix} \frac{\partial z^\star}{\partial y} \\ \frac{\partial \lambda^\star}{\partial y} \\ \frac{\partial \nu^\star}{\partial y} \end{bmatrix} = - \begin{bmatrix} q(z^\star, \nu^\star, \lambda^\star) \\ c(z^\star, \lambda^\star) \\ b(z^\star) \end{bmatrix}, \tag{8}$$

$D(\cdot) : \mathbb{R}^m \to \mathbb{R}^{m\times m}$ represents a diagonal matrix that formed from a vector and $z^\star, \nu^\star, \lambda^\star$ denotes the optimal primal and dual variables. Left-hand side is the KKT matrix of the original optimization problem times the Jacobian matrix of primal and dual variables to the omitted parameter y, e.g., $\frac{\partial z^\star}{\partial y} \in \mathbb{R}^{p\times d}$. Right-hand side is the negative partial derivatives of KKT conditions to the y.

We can then backpropagate losses by solving the linear system in Eq. (8). In practice, however, explicitly computing the actual Jacobian matrices $\frac{\partial z^\star}{\partial y}$ is not desirable due to space complexity; instead, [8] products previous pass gradient vectors $\frac{\partial \mathcal{L}}{\partial z^\star} \in \mathbb{R}^d$, to reform it by notations $[\tilde{z} \in \mathbb{R}^d, \tilde{\lambda} \in \mathbb{R}^m, \tilde{\nu} \in \mathbb{R}^n]$ (see Appendix 7.2):

$$\begin{bmatrix} P(z^\star, \nu^\star, \lambda^\star) & G(z^\star)^\top & A(z^\star)^\top \\ D\left(\lambda^\star\right) G(z^\star) & D\left(g(x^\star)\right) & 0 \\ A(z^\star) & 0 & 0 \end{bmatrix} \begin{bmatrix} \tilde{z} \\ \tilde{\lambda} \\ \tilde{\nu} \end{bmatrix} = - \begin{bmatrix} (\frac{\partial \mathcal{L}}{\partial z^\star})^\top \\ 0 \\ 0 \end{bmatrix}. \tag{9}$$

And the direct gradients $\nabla_y \mathcal{L} \in \mathbb{R}^p = [q(z^\star, \nu^\star, \lambda^\star), c(z^\star, \lambda^\star), b(z^\star)][\tilde{z}, \tilde{\lambda}, \tilde{\nu}]^\top$.

4 Methodology

4.1 Backward Pass as QPs

Our method solves Eq. (9) using reformulation method. Consider a general class of QPs that have d decision variables, n equality constraints and m inequality constraints:

$$\underset{\tilde{z}}{\text{minimize}}\ \frac{1}{2}\tilde{z}^\top P\tilde{z} + q^\top \tilde{z} \quad s.t.\ A\tilde{z} = b,\ G\tilde{z} \leq c, \tag{10}$$

where $P \in \mathbb{S}_+^d$, $q \in \mathbb{R}^d$, $A \in \mathbb{R}^{n\times d}$, $b \in \mathbb{R}^n$, $G \in \mathbb{R}^{m\times d}$ and $c \in \mathbb{R}^m$. KKT conditions write down in matrix form:

$$\begin{bmatrix} P & G^\top & A^\top \\ D(\tilde{\lambda})G & D(G\tilde{z}-c) & 0 \\ A & 0 & 0 \end{bmatrix} \begin{bmatrix} \tilde{z} \\ \tilde{\lambda} \\ \tilde{\nu} \end{bmatrix} = \begin{bmatrix} -q \\ D(\tilde{\lambda})c \\ b \end{bmatrix}. \tag{11}$$

We note that Eq. (11) is quivalent to Eq. (9) if and only if: (i) $P = P(z^\star, \nu^\star, \lambda^\star),\ A = A(z^\star),\ D(\tilde{\lambda})G = D(\lambda^\star)G(z^\star)$, $[-q, D(\tilde{\lambda})c, b] = [-\left(\frac{\partial \mathcal{L}}{\partial z^\star}\right)^\top, 0, 0]$ and (ii) $P(z^\star, \nu^\star, \lambda^\star)$ is positive semi-definite. As backward pass solves after forward pass, we can change inequality constraints to an accurate active-set (i.e., a set of binding constraints) of equality conditions, and then condition (i) always holds for equality-constrained QP. From this, the following theorem can be obtained

Theorem 1 *Suppose that the convex optimization 1 is not primal infeasible and the corresponding Jacobian vector $\nabla_y \mathcal{L}$ exists. It is given by $\nabla_y \mathcal{L} = [q(z^\star, \nu^\star, \lambda^\star), c(z^\star, \lambda^\star), b(z^\star)][\tilde{z}, \tilde{\lambda}, \tilde{\nu}]^\top$ and $\tilde{z}, \tilde{\lambda}, \tilde{\nu}$ is the optimal solution of following equality constrained Quadratic Problem:*

$$\underset{\tilde{z}}{\text{minimize}}\ \frac{1}{2}\tilde{z}^\top P\tilde{z} + q^\top \tilde{z} \quad \textit{s.t.}\ A\tilde{z} = b,\ G_+\tilde{z} = c_+. \tag{12}$$

Where $P = P(z^\star, \nu^\star, \lambda^\star),\ A = A(z^\star),\ G_+ = G_+(z^\star)$ and $[-q, c_+, b] = [-\left(\frac{\partial \mathcal{L}}{\partial z^\star}\right)^\top, 0, 0]$. G_+, c_+ has the same row of active-set as original inequality constraints.

Though our BPQP procedure described above also stands for Jacobians with forms other than vectors, e.g., matrices, in these cases where each 1-dimension column in $[\tilde{z}, \tilde{\lambda}, \tilde{\nu}]^\top$ right multiply the same KKT matrix and can be viewed as QPs packed in multi-dimensions, directly calculating the *inverse* of the KKT matrix may be more appropriate, especially when it contains a special structure like OptNet [8] and SATNet [26].

General Gradients The intuition of BPQP is that the linearity of IFT requires the KKT matrix left-multiply homogeneous linear partial derivative variables. Theorem 1 highlights a special situation that considers gradients at the optimal point (KKT conditions are satisfied). Generally, BPQP provides perspective to define gradients in parameter-solution space that preserves KKT norm. Let us consider a series of vectors denoting the kth iteration norm value of KKT conditions:

$$\|r^{(k)}\| = \| \left(r_{dual}^{(k)}, r_{cent}^{(k)}, r_{prim}^{(k)}\right) \| = C_k. \tag{13}$$

Where $r^{(k)} \in \mathbb{R}^{d+m+n}$ the KKT conditions in kth iteration and $C_k \in \mathbb{R}$ the norm value. The series $\{C_0, C_1, ..., C_k\}$ converges to 0 if the iteration algorithm is a contraction operator. Let $\mathcal{Q}^{(k)}$ denote standard QP problem w.r.t. parameter $P_k, q_k, A_k, b_k, G_k, c_k$ and decision variable z_k. At each iteration, BPQP yields $\nabla_y \mathcal{L}^{(k)}$ that preserves $\|r^{(k)}\| = C_k$. (See in Appendix 7.3)

Time Complexity The time complexity of solving such QP is $\mathcal{O}(N^3)$ in the number of variables and constraints which is at the same level as directly solving the linear system Eq. (9). However, reformulation as QP provides substantial structures that can be exploited for efficiency, such that (we cover them in Section 4.2) sparse matrix, solution polishing [12], active-sets, and first-order methods, etc. Cleverly implement BPQP, experiments at fairly large-scale dimensions in practice highlight BPQP's capacity in comparison to the state-of-art differentiable solver and NN-based optimization layers. Intuitively, BPQP is more efficient than previous methods because it utilizes the convex QP structural trait in the backward pass.

4.2 Efficiently Solve Backward Pass Problem with OSQP

The solver we referenced is OSQP [12], which incorporates the sparse matrix method and uses a first-order Alternating Direction Method of Multipliers (ADMM) method to solve QPs. We summarize OSQP here [27]. On each iteration, it refines a solution from an initialization point for vectors $z^{(0)} \in \mathbb{R}^d,\ \lambda^{(0)} \in \mathbb{R}^m$, and $\nu^{(0)} \in \mathbb{R}^n$. And then iteratively computes the values for the $k+1$th iterates by solving the following linear system:

$$\begin{bmatrix} P+\sigma I & A^\top \\ A & \mathrm{diag}(\rho)^{-1} \end{bmatrix} \begin{bmatrix} z^{(k+1)} \\ v^{(k+1)} \end{bmatrix} = \begin{bmatrix} \sigma z^{(k)} - q \\ \lambda^{(k)} - \mathrm{diag}(\rho)^{-1}\nu^{(k)} \end{bmatrix}, \tag{14}$$

And then performing the following updates:

$$\begin{aligned} \tilde{\lambda}^{(k+1)} &\leftarrow \lambda^{(k)} + \mathrm{diag}(\rho)^{-1}\left(v^{(k+1)} - \nu^{(k)}\right) \\ \lambda^{(k+1)} &\leftarrow \Pi\left(\tilde{\lambda}^{(k+1)} + \mathrm{diag}(\rho)^{-1}\nu^{(k)}\right) \\ \nu^{(k+1)} &\leftarrow \nu^{(k)} + \mathrm{diag}(\rho)\left(\tilde{\lambda}^{(k+1)} - \lambda^{(k+1)}\right) \end{aligned}, \tag{15}$$

where $\sigma \in \mathbb{R}_+$ and $\rho \in \mathbb{R}^n_+$ are the *step-size* parameters, and $\Pi : \mathbb{R}^m \to \mathbb{R}^m$ denotes the Euclidean projection onto constraints set. When the primal and dual residual vectors are small enough in norm after kth iterations, $z^{(k+1)}$, $\lambda^{(k+1)}$ and $\nu^{(k+1)}$ converges to exact solution $z^\star$, $\lambda^\star$ and $\nu^\star$.

In particular, given a backward pass problem Eq. (12) with known active constraints, as stated in OSQP, we form a KKT matrix below[1]:

$$\begin{bmatrix} P+\delta I & G_+^\top & A^\top \\ G_+ & -\delta I & 0 \\ A & 0 & -\delta I \end{bmatrix} \begin{bmatrix} \tilde{z} \\ \tilde{\lambda}_+ \\ \tilde{\nu} \end{bmatrix} = \begin{bmatrix} -q \\ 0 \\ 0 \end{bmatrix}, \tag{16}$$

As the original KKT matrix is not always solvable, e.g., if it has one or more redundant constraints, we modify it to be more robust for QPs of all kinds by adding a small regularization parameter $D(P+\delta I, -\delta I, -\delta I)$ (in Eq. (16)) as default $\delta \approx 10^{-6}$. We could then solve it with the aforementioned ADMM procedure to obtain a candidate solution, denoted as $\hat{t}$ and recover the exact solution t from the perturbed KKT conditions $(K+\Delta K)\hat{t} = g$ by iteratively solving:

$$(K+\Delta K)\Delta\hat{t}^k = g - K\hat{t}^k. \tag{17}$$

where $\hat{t}^{k+1} = \hat{t}^k + \Delta\hat{t}^k$ and it converges to t very quickly in practice[12] for only one backward- and one forward-solve. Thus our BPQP method solves backward pass problems in a general but efficient way.

4.3 Example: Differentiable QP and SOCP

Below we provide examples for differentiable QP and SOCP oracles (i.e. solutions) using BPQP. The general procedure is to first write down KKT matrix of the original decision making problem. And then apply Theorem 1. Assuming the optimal solution $z^\star$ is already obtained in forward pass.

Differentiable QP With a slight abuse of notation, given the standard QP problem with parameters P, q, A, b, G, c as in Eq. (10). The result is exactly the same as OptNet [8] since both approaches are for accurate gradients. But BPQP is capable of efficiently solving large-scale QP forward-backward pass via ADMM [12], as shown in Section 5.1.

$$\begin{array}{lll} \nabla_Q\mathcal{L} = \frac{1}{2}\left(\tilde{z}z^{\star T} + z^\star\tilde{z}^T\right) & \nabla_q\mathcal{L} = \tilde{z} & \nabla_A\mathcal{L} = \tilde{\nu}z^{\star T} + \nu^\star\tilde{z}^T \\ \nabla_b\mathcal{L} = -\tilde{\nu} & \nabla_{G_+}\mathcal{L} = D(\lambda^\star_+)\tilde{\lambda}z^{\star T} + \lambda^\star_+\tilde{z}^T & \nabla_{c_+}\mathcal{L} = -D(\lambda^\star_+)\tilde{\lambda} \end{array} \tag{18}$$

And $[\tilde{z}, \tilde{\nu}, \tilde{\lambda}]$ solves

$$\underset{\tilde{z}}{\text{minimize}}\ \frac{1}{2}\tilde{z}^\top P\tilde{z} + \frac{\partial\mathcal{L}}{\partial z^\star}^\top \tilde{z} \quad \text{s.t. } A\tilde{z} = 0,\ G_+\tilde{z} = 0. \tag{19}$$

[1] $G_+ = G(z^\star_+)$ has the same row of active-set as $g(z^\star_+) = 0,\ z \in \mathbb{R}^{m_+}$. m_+ is the number of active sets.

Differentiable SOCP The second-order cone programming (SOCP) of our interest is the problem of robust linear program [28]:

$$\underset{z}{\text{minimize}}\ q^\top z \quad \text{s.t. } a_i^\top z + \|z\|_2 \leq b_i\ i = 1, 2, ..., m. \tag{20}$$

where $q \in \mathbb{R}^d$, $a_i \in \mathbb{R}^d$, and $b_i \in \mathbb{R}$. With m inequality constraints in $L2$ norm, we give the gradients w.r.t. above parameters.

$$\nabla_q \mathcal{L} = \tilde{z} \quad \nabla_{a_{i+}} \mathcal{L} = \lambda^\star_{i+}\tilde{z} + \lambda^\star_{i+}\tilde{\lambda}_i z^\star \quad \nabla_{c_{i+}} \mathcal{L} = \tilde{\lambda}_i,\ i = 1, 2, ..., m. \tag{21}$$

And $[\tilde{z}, \tilde{\nu}, \tilde{\lambda}]$ are given by ($t_1 = \sum_i \lambda^\star_{i+}$ and $t_0 = \|z^\star\|_2$)

$$\underset{\tilde{z}}{\text{minimize}}\ \frac{1}{2}\tilde{z}^\top \left(\frac{t_1}{t_0}\mathbb{I} - \frac{t_1}{t_0^3} z^\star z^{\star\top}\right)\tilde{z} + \frac{\partial \mathcal{L}}{\partial z^\star}\tilde{z} \quad \text{s.t. } (a_{i+}^\top + \frac{1}{t_0}z^\star)^T\tilde{z} = 0,\ i = 1, 2, ..., m. \tag{22}$$

5 Experiments

In this section, we present several experimental results that highlight the capacities of the BPQP. To be precise, we evaluate for (i) large-scale computational efficiency over existing solvers on random-generated constrained optimization problems including QP, LP, and SOCP, and (ii) performance on real-world end-to-end portfolio optimization task that is challenging for existing predict-then-optimize approaches.

5.1 Simulated Large-scale Constrained Optimization

We randomly generate three datasets (e.g. simulated constrained optimization) for QPs, LPs, and SOCPs respectively. The datasets cover diverse scales of problems. The problem scale includes 10×5, 50×10, 100×20, 500×100 (e.g., 10×5 represents the scale of 10 variables, 5 equality constraints, and 5 inequality constraints).

QPs Dataset The format of generated QPs follows Eq. (12) to which the notations in the following descriptions align. We take q as the learnable parameter to be differentiated and $\mathcal{L} = \mathbf{1}^\top z^\star$ in Eq. (9). To generate a positive semi-definite matrix P, ${P'}^\top P' + \delta I$ is assigned to P where $P' \in \mathbb{R}^{d\times d}$is a randomly generated dense matrix, δI is a small regularization matrix, and $\delta = 10^{-6}$. Potentially, we set $c = Gz',\ G \in \mathbb{R}^{m\times n},\ z' \in \mathbb{R}^n$ to avoid large slackness values that lead to inaccurate results. All other random variables are drawn i.i.d. from unit uniform distribution $U(0, 1)$.

LPs Dataset The LP problems are generated in the format below

$$\underset{z}{\text{minimize}}\ \theta^T z + \epsilon\|z\|_2^2 \ \text{ s.t. } Az = b, Gz \leq h. \tag{23}$$

where $\theta \in \mathbb{R}^d$ is the learnable parameter to be differentiated, $z \in \mathbb{R}^d$, $A \in \mathbb{R}^{n\times d}$, $b \in \mathbb{R}^n$, $G \in \mathbb{R}^{m\times d}$, $h \in \mathbb{R}^m$ and $\epsilon \in \mathbb{R}_+$. All random variables are drawn from the same distribution as the QPs dataset. It is noteworthy that it contains an extra item $\epsilon\|z\|_2^2$ compared with traditional LP. This item is added to make the optimal solution $z^\star$ differentiable with respect to θ. Without this item, $P(z^\star, \nu^\star, \lambda^\star)$ is always zero and thus the left-hand side matrix becomes singular in Eq. (8). This is a trick adopted by previous work [2]. CVXPY will reformulate the problem to a cone program and can handle this issue internally. So ϵ is set to 0 for CVXPY. For other differentiable optimizers, $\epsilon = 10^{-6}$ as default.

SOCPs Dataset For SOCP in Eq. (20), we consider a specific simple case, i.e. $a_i = 0\ \forall i$ and this relaxations results in $m = 1$. As in QP and LP, we take q as differentiable parameter and set loss function $\mathcal{L} = \mathbf{1}^\top z^\star$, but all variables are drawn i.i.d. from standard Gaussian distribution $N(0, 1)$.

Compared Methods To demonstrate the effectiveness of BPQP, we evaluate the efficiency and accuracy of state-of-the-art differentiable convex optimizers, as well as **BPQP**, on the datasets mentioned above. The following methods are compared: **CVXPY** [17], **qpth/OptNet** [8], and **Exact**. Exact adopts the same algorithm as BPQP for the forward pass, but attempts to calculate exact gradients using direct matrix inversion on the KKT matrix during the backward pass.

Evaluation and Metrics To evaluate the efficiency of the compared methods, the runtime in seconds is used for each forward pass, backward pass, and total process. To evaluate the accuracy, we first get a target solution z^{Exact} with a high-accuracy method and then calculate the L_2-distance from

dataset	metric	pass size method	Backward 10×5	 50×10	 100×20	 500×100	Total(Forward + Backward) 10×5	 50×10	 100×20	 500×100
QP	abs. time	Exact	40.6(±60.3)	325.4(±280.7)	3388.8(±540.6)	37279.4(±2503.0)	41.7(±60.2)	333.7(±280.5)	3440.1(±543.4)	38796.1(±2530.2)
	(scale 1.0e-04)	CVXPY	39.5(±19.1)	75.2(±17.1)	-	-	472.6(±143.2)	37611.1(±1430.3)	-	-
		qpth/OptNet	33.3(±9.8)	35.9(±8.9)	38.3(±12.3)	-	851.6(±499.4)	952.8(±201.0)	1308.2(±238.0)	-
		BPQP	**0.5(±0.1)**	**2.6(±0.5)**	**10.5(±8.4)**	**116.2(±20.4)**	**1.6(±0.6)**	**10.9(±5.4)**	**61.8(±35.3)**	**1632.9(±223.7)**
LP	abs. time	Exact	1.2(±2.0)	19.5(±12.4)	240.5(±36.4)	2955.6(±131.7)	1.3(±2.0)	19.8(±12.4)	242.7(±36.4)	3025.6(±133.5)
	(scale 1.0e-03)	CVXPY	4.3(±2.8)	3.7(±1.0)	6.1(±2.2)	25.9(±2.9)	28.3(±9.0)	26.1(±6.4)	45.3(±13.6)	302.1(±20.7)
		qpth/OptNet	3.9(±1.1)	3.7(±1.1)	4.0(±1.0)	5.9(±0.9)	112.2(±24.3)	106.3(±25.6)	116.1(±23.0)	248.5(±58.5)
		BPQP	**0.1(±0.8)**	**0.1(±0.0)**	**0.6(±1.3)**	**4.8(±0.8)**	**0.2(±0.9)**	**0.5(±0.2)**	**2.8(±1.5)**	**74.7(±21.4)**
SOCP	abs. time	Exact	2.3(±5.1)	4.2(±6.3)	12.6(±23.2)	110.7(±116.8)	47.6(±6.9)	52.0(±6.7)	73.4(±23.6)	300.3(±117.1)
	(scale 1.0e-04)	CVXPY	8.8(±0.9)	8.9(±0.3)	9.0(±0.6)	**11.1(±0.3)**	64.1(±5.1)	80.1(±3.4)	105.0(±2.9)	334.3(±3.2)
		BPQP	**0.2(±0.0)**	**0.7(±0.0)**	**2.3(±0.0)**	53.4(±0.3)	**45.4(±4.9)**	**48.5(±2.6)**	**63.1(±1.6)**	**242.9(±2.7)**

Table 1: Efficiency evaluation of methods by runtime in seconds based on 200 runs, with lower numbers indicating better performance.

compared methods(Err. $= \|z^{\text{Exact}} - z^{\text{method}_i}\|_2$). We run each instance 200 times for average and standard deviation (marked in brackets) of the metrics.

Results The results for efficiency evaluation are shown in Table 1. The evaluation covers three typical optimization problems with different problem scales. The results start from the QP dataset. Compared with state-of-the-art accurate methods, CVXPY and qpth/OptNet, BPQP achieves tens to thousands of times of speedup in total time. When the problem becomes large like 500×100, previous methods fail to generate results due to known issues[2]. CVXPY is extremely much slower because it reformulates the QP as a conic program and the reformulation is slow and has to be done repeatedly when the problem parameters change [12]. It is worth noting that BPQP is faster even in the backward pass, where CVXPY and qpth/OptNet share information from the forward pass to reduce computational costs. Sharing this information will limit the available forward solvers and result in a coupled design. Exact falls back to a simpler implementation that does not involve sharing information between designs. It solves the KKT matrix (i.e., Eq. (9)) in the backward pass via a matrix inverse method without relying on information from the forward pass. Although Exact uses a relatively efficient implementation in the forward pass (i.e., a first-order method, same as BPQP), the fallback backward implementation becomes a bottleneck for efficiency. The results of the LP dataset lead to similar conclusions as those of the QP dataset.

In the evaluation of the SOCP dataset, qpth/OptNet focuses on QP and is excluded from this non-QP setting. Due to the specialty of SOCP, CVXPY does not require problem reformulation into conic programs, giving it an advantage. BPQP still outperforms other options in terms of total time across all problem scales.

Table 2: Backward accuracy of methods on simulated QP and non-QP(SOCP) dataset

method	QP BPQP	 CVXPY	 qpth/OptNet	SOCP BPQP	 CVXPY
Avg. Err.	**1.15e-04(±7.10e-04)**	2.12e-02(±3.30e-02)	1.72e-03(±4.88e-03)	3.03e-07(±6.36e-08)	**1.18e-07(±2.70e-07)**

The accuracy evaluation results are shown in Table 1. In the forward pass, all solvers give nearly the same results ($Err.$ is below 10^{-4}), which is not shown in the table. When evaluating the backward accuracy, we use a matrix inverse method with high precision to solve Eq. (9) directly to get a target solution(i.e. z^{Exact}) and compare solutions from evaluated methods against it. The $Err.$ is relatively higher than that in the forward pass due to accumulated computational errors. Among them, the error of our method BPQP is the lowest in QP. The $Err.$ of all methods are small enough for SOCP.

5.2 Real-world End-to-End Portfolio Optimization

Portfolio optimization is a fundamental problem for asset allocation in finance. It involves constructing and balancing the investment portfolio periodically to maximize profit and minimize risk. We now show how to apply BPQP to the problem of end-to-end portfolio optimization.

Mean-Variance Optimization (MVO) [29] is a basic portfolio optimization model that maximizes risk-adjusted returns and requires long only and budget constraints. It can be formulated as

$$\underset{w}{\text{maximize}}\ \mu^\top w - \frac{\gamma}{2} w^\top \Sigma w \ \text{ subject to } \ \mathbf{1}^\top w = 1,\ w \geq 0. \tag{24}$$

[2] `https://github.com/locuslab/qpth/issues/37`

where variables $w \in \mathbb{R}^d$ represent the portfolio weight, $\gamma \in \mathbb{R} > 0$, the risk aversion coefficient, and $\mu \in \mathbb{R}^d$ the expected returns to be predicted. We built an ML predictor to approximate expected returns. The covariance matrix, Σ, of all assets can be learned end-to-end by BPQP. However, it preserves a more stable characteristic than returns in time-series [30]. Therefore, we set it as a constant.

Benchmarks We evaluate BPQP based on the most widely used predictive baseline neural network, MLP. For the learning approach, we compared the separately two-stage(**Two-Stage**) and end-to-end learning approaches. For end-to-end learning approaches, we compare both accurate(**BPQP**) and approximate(a learn-to-optimise approach, **DC3**[19]) predict-then-optimize learning approaches. The optimization problem in the experiment has a variable scale of 500, which cannot be handled by other layers based on CVXPY and qpth/OptNet. Our implementation substantially lowers the barrier to using convex optimization layers. For large-scale real-world scenarios, approximate methods such as DC3 can be a practical solution in terms of efficiency and are thus listed in the results.

Table 3: Prediction and decision(portfolio) metrics evaluation of different methods in portfolio optimization. Lower is better for MSE, while greater is better for other metrics.

	Prediction Metrics			Portfolio Metrics	
	MSE	IC	ICIR	Ann.Ret.(%)	Sharpe
Two-Stage	**0.034(±0.006)**	**0.033(±0.004)**	**0.32(±0.03)**	9.28(±3.46)	0.65(±0.25)
DC3	0.034(±0.003)	0.033(±0.001)	0.31(±0.01)	-0.40(±0.97)	-0.16(±0.60)
BPQP	0.061(±0.008)	0.026(±0.002)	0.28(±0.03)	**17.67(±6.11)**	**1.28(±0.43)**

Results The overall results are shown in Table 3. As we can see in the prediction metrics, Two-Stage performs best. Instead of minimizing multiple objectives without a non-competing guarantee, Two-Stage only focuses on minimizing the prediction error and thus avoids the trade-off between different objectives. However, achieving the best prediction performance does not equal the best decision performance. BPQP outperforms Two-Stage in all decision metrics, although its prediction performance is slightly compromised. These experiments demonstrate the superiority of end-to-end learning, which minimizes the ultimate decision error, over separate two-stage learning. DC3 is an approximate learning-to-optimize end-to-end learning approach. Although DC3 is computationally efficient and thus applicable to large-scale real-world datasets, it performs poorly in most metrics. This is due to the inaccurate gradient that deteriorates the learned model based on DC3. Therefore, accuracy is an important feature in end-to-end learning.

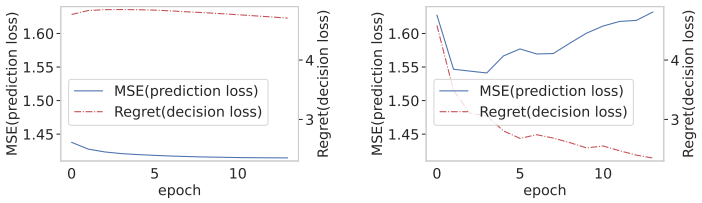

(a) Two-Stage (b) BPQP

Figure 2: The prediction and decision error/loss of methods with different objectives

To gain a deeper understanding of how end-to-end regret loss works, Figure 2 demonstrates the detailed learning curve of Two-Stage and BPQP. For each subfigure, the x-axis represents the number of epochs during training, and the y-axis represents the training loss of prediction and decision, respectively. Two-Stage aims to minimize the prediction loss, which is ultimately smaller than BPQP. However, the decision loss remains at a high level, resulting in a suboptimal decision. BPQP aims to minimize both prediction loss and decision loss. Both losses decrease initially, and then they start to compete in the later epochs. However, the decision error remains at a much lower value than Two-Stage, resulting in better decisions in the final evaluation.

6 Conclusion and Future Works

We have introduced a differentiable convex optimization framework for efficient end-to-end learning. Previous work shared gradient information between the forward pass and backward pass, which

limited the choice of optimization algorithms and made it difficult to achieve overall efficiency. To address this, we solve the forward and backward passes in a "decoupled" manner. This enables the use of any optimization algorithms that best match the problem structure and allows for large-scale training. We conducted extensive experiments to demonstrate the efficiency of BPQP. Our work is the first to apply the predict-then-optimize paradigm in a large-scale, real-world application. The final results show that BPQP significantly improves decision performance in real-world scenarios.

Limitations Compared to the quadratic complexity of standard feedforward layers, solving optimization problems exactly has a cubic time complexity. Therefore, it is preferable to use approximated solutions and gradients while avoiding biased gradients. BPQP uses external solvers [12, 17, 7, 31] that are specialized for solving certain types of convex programs. However, these solvers are typically implemented using CPU resources. It is possible to achieve even faster performance for specific types of decision-making problems using GPU-based solvers [8]. These limitations are important directions for future works.

References

[1] A. N. Elmachtoub and P. Grigas, "Smart "predict, then optimize"," *Management Science*, vol. 68, no. 1, pp. 9–26, 2022.

[2] B. Wilder, B. Dilkina, and M. Tambe, "Melding the data-decisions pipeline: Decision-focused learning for combinatorial optimization," in *Proceedings of the AAAI Conference on Artificial Intelligence*, vol. 33, no. 01, 2019, pp. 1658–1665.

[3] H. Liu and P. Grigas, "Risk bounds and calibration for a smart predict-then-optimize method," *Advances in Neural Information Processing Systems*, vol. 34, pp. 22 083–22 094, 2021.

[4] J. Kotary, F. Fioretto, P. Van Hentenryck, and B. Wilder, "End-to-end constrained optimization learning: A survey," *arXiv preprint arXiv:2103.16378*, 2021.

[5] J. Mandi, P. J. Stuckey, T. Guns *et al.*, "Smart predict-and-optimize for hard combinatorial optimization problems," in *Proceedings of the AAAI Conference on Artificial Intelligence*, vol. 34, no. 02, 2020, pp. 1603–1610.

[6] A. Agrawal, S. Barratt, S. Boyd, E. Busseti, and W. M. Moursi, "Differentiating through a cone program," *arXiv preprint arXiv:1904.09043*, 2019.

[7] A. Agrawal, B. Amos, S. Barratt, S. Boyd, S. Diamond, and J. Z. Kolter, "Differentiable convex optimization layers," *Advances in neural information processing systems*, vol. 32, 2019.

[8] B. Amos and J. Z. Kolter, "Optnet: Differentiable optimization as a layer in neural networks," in *International Conference on Machine Learning*. PMLR, 2017, pp. 136–145.

[9] M. F. Tappen, C. Liu, E. H. Adelson, and W. T. Freeman, "Learning gaussian conditional random fields for low-level vision," in *2007 IEEE Conference on Computer Vision and Pattern Recognition*. IEEE, 2007, pp. 1–8.

[10] P. Donti, B. Amos, and J. Z. Kolter, "Task-based end-to-end model learning in stochastic optimization," *Advances in neural information processing systems*, vol. 30, 2017.

[11] G. Ifrim, B. O'Sullivan, and H. Simonis, "Properties of energy-price forecasts for scheduling," in *Principles and Practice of Constraint Programming: 18th International Conference, CP 2012, Québec City, QC, Canada, October 8-12, 2012. Proceedings*. Springer, 2012, pp. 957–972.

[12] B. Stellato, G. Banjac, P. Goulart, A. Bemporad, and S. Boyd, "Osqp: An operator splitting solver for quadratic programs," *Mathematical Programming Computation*, vol. 12, no. 4, pp. 637–672, 2020.

[13] M. Frank and P. Wolfe, "An algorithm for quadratic programming," *Naval research logistics quarterly*, vol. 3, no. 1-2, pp. 95–110, 1956.

[14] P.-L. Lions and B. Mercier, "Splitting algorithms for the sum of two nonlinear operators," *SIAM Journal on Numerical Analysis*, vol. 16, no. 6, pp. 964–979, 1979.

[15] D. Gabay and B. Mercier, "A dual algorithm for the solution of nonlinear variational problems via finite element approximation," *Computers & mathematics with applications*, vol. 2, no. 1, pp. 17–40, 1976.

[16] P. Wolfe, "The simplex method for quadratic programming," *Econometrica: Journal of the Econometric Society*, pp. 382–398, 1959.

[17] S. Diamond and S. Boyd, "Cvxpy: A python-embedded modeling language for convex optimization," *The Journal of Machine Learning Research*, vol. 17, no. 1, pp. 2909–2913, 2016.

[18] B. O'donoghue, E. Chu, N. Parikh, and S. Boyd, "Conic optimization via operator splitting and homogeneous self-dual embedding," *Journal of Optimization Theory and Applications*, vol. 169, pp. 1042–1068, 2016.

[19] P. L. Donti, D. Rolnick, and J. Z. Kolter, "Dc3: A learning method for optimization with hard constraints," *arXiv preprint arXiv:2104.12225*, 2021.

[20] C. K. Joshi, Q. Cappart, L.-M. Rousseau, and T. Laurent, "Learning the travelling salesperson problem requires rethinking generalization," *Constraints*, pp. 1–29, 2022.

[21] E. Khalil, H. Dai, Y. Zhang, B. Dilkina, and L. Song, "Learning combinatorial optimization algorithms over graphs," *Advances in neural information processing systems*, vol. 30, 2017.

[22] Q. Ma, S. Ge, D. He, D. Thaker, and I. Drori, "Combinatorial optimization by graph pointer networks and hierarchical reinforcement learning," *arXiv preprint arXiv:1911.04936*, 2019.

[23] W. Kool, H. Van Hoof, and M. Welling, "Attention, learn to solve routing problems!" *arXiv preprint arXiv:1803.08475*, 2018.

[24] A. S. Uysal, X. Li, and J. M. Mulvey, "End-to-end risk budgeting portfolio optimization with neural networks," *arXiv preprint arXiv:2107.04636*, 2021.

[25] H. Chen, P. Wang, F. Wang, W. Tian, L. Xiong, and H. Li, "Epro-pnp: Generalized end-to-end probabilistic perspective-n-points for monocular object pose estimation," in *Proceedings of the IEEE/CVF Conference on Computer Vision and Pattern Recognition*, 2022, pp. 2781–2790.

[26] P.-W. Wang, P. Donti, B. Wilder, and Z. Kolter, "Satnet: Bridging deep learning and logical reasoning using a differentiable satisfiability solver," in *International Conference on Machine Learning*. PMLR, 2019, pp. 6545–6554.

[27] J. Ichnowski, P. Jain, B. Stellato, G. Banjac, M. Luo, F. Borrelli, J. E. Gonzalez, I. Stoica, and K. Goldberg, "Accelerating quadratic optimization with reinforcement learning," *Advances in Neural Information Processing Systems*, vol. 34, pp. 21 043–21 055, 2021.

[28] K. P. Bennett and O. L. Mangasarian, "Robust linear programming discrimination of two linearly inseparable sets," *Optimization methods and software*, vol. 1, no. 1, pp. 23–34, 1992.

[29] H. M. Markowitz, "Portfolio selection," *The journal of finance*, vol. 7, no. 1, p. 77–91, 1952.

[30] T. Lux and M. Marchesi, "Volatility clustering in financial markets: a microsimulation of interacting agents," *International journal of theoretical and applied finance*, vol. 3, no. 04, pp. 675–702, 2000.

[31] A. Domahidi, E. Chu, and S. Boyd, "Ecos: An socp solver for embedded systems," in *2013 European control conference (ECC)*. IEEE, 2013, pp. 3071–3076.

[32] B. O'Donoghue, E. Chu, N. Parikh, and S. Boyd, "Conic optimization via operator splitting and homogeneous self-dual embedding," *Journal of Optimization Theory and Applications*, vol. 169, no. 3, pp. 1042–1068, June 2016. [Online]. Available: http://stanford.edu/~boyd/papers/scs.html

[33] B. O'Donoghue, "Operator splitting for a homogeneous embedding of the linear complementarity problem," *SIAM Journal on Optimization*, vol. 31, pp. 1999–2023, August 2021.

[34] X. Yang, W. Liu, D. Zhou, J. Bian, and T.-Y. Liu, "Qlib: An ai-oriented quantitative investment platform," *arXiv preprint arXiv:2009.11189*, 2020.

[35] E. Beyaz, F. Tekiner, X.-j. Zeng, and J. Keane, "Comparing technical and fundamental indicators in stock price forecasting," in *2018 IEEE 20th International Conference on High Performance Computing and Communications; IEEE 16th International Conference on Smart City; IEEE 4th International Conference on Data Science and Systems (HPCC/SmartCity/DSS)*. IEEE, 2018, pp. 1607–1613.

7 Supplementary Material

7.1 MAP Predict-then-optimize Loss

On selecting β for portfolio optimization in section 5.2, mathematically $\beta = \frac{\sigma_r^2}{\sigma_y^2} \in (0, 1)$ denotes the ratio of variances between the random parameter y and the regret. Since the empirical regret suffers a more severe fluctuation over y ($\sigma_r \gg \sigma_y > 0$) in convex optimization [5], prediction error should dominate in the end-to-end loss, however, we use an empiric distribution to approximate the Dirac distribution and set β to a small ($\beta = 0.1$ in portfolio optimization experiment) but not zero value.

Under normality assumption

$$\arg\max(p(\theta \mid \text{regret}, y, x)) \propto$$
$$\arg\max \prod_i \frac{1}{\sigma_r\sqrt{2\pi}} e^{-\frac{\text{regret}_i^2}{2\sigma_r^2}} \times \prod_j \frac{1}{\sigma_y\sqrt{2\pi}} e^{-\frac{(y_j - \hat{y}_j)_j^2}{2\sigma_y^2}}, \tag{25}$$

That is

$$\arg\min \sum_i regret_i^2 + \frac{\sigma_r^2}{\sigma_y^2} \sum_j (y_j - \hat{y}_j)^2. \tag{26}$$

7.2 Differentiate Through KKT Conditions Using the Implicit Function Theorem

In this section, we give a detailed discussion on Eq. (9). The sufficient and necessary conditions for optimality for Eq. (1) are KKT conditions:

$$\begin{aligned} \nabla f(z^\star) + \nabla h(z^\star)\nu^\star + \nabla g(z^\star)\lambda^\star &= 0 \\ h(z^\star) &= 0 \\ D\left(\lambda^\star\right)\left(g(z^\star)\right) &= 0 \\ \lambda^\star &\geq 0, \end{aligned} \tag{27}$$

Applying the Implicit Function Theorem to the KKT conditions and let $P(z^\star, \nu^\star, \lambda^\star) = \nabla^2 f(z^\star) + \nabla^2 h(z^\star)\nu^\star + \nabla^2 g(z^\star)\lambda^\star$, $A(z^\star) = \nabla h(z^\star)$ and $G(z^\star) = \nabla g(z^\star)$ yields to Eq. (8). We can then backpropagate losses by solving the linear system. In practice, however, explicitly computing the actual Jacobian matrices $\frac{\partial z^\star}{\partial y}$ is not desirable due to space complexity; instead, we product some previous pass gradient vectors $\frac{\partial \mathcal{L}}{\partial z^\star} \in \mathbb{R}^d$, to reform it by noting that

$$\nabla_y \mathcal{L} = \left[\frac{\partial z^\star}{\partial y},\ \frac{\partial \lambda^\star}{\partial y},\ \frac{\partial \nu^\star}{\partial y}\right] \begin{bmatrix} \left(\frac{\partial \mathcal{L}}{\partial z^\star}\right)^\top \\ 0 \\ 0 \end{bmatrix}, \tag{28}$$

The first term of left hand side is the transposed solution of Eq. (8) and above can be reformulated as

$$\nabla_y \mathcal{L} = [q,\ c,\ b] \underbrace{\begin{bmatrix} P(z^\star, \nu^\star, \lambda^\star) & D\left(\lambda^\star\right) G(z^\star) & A(z^\star) \\ G(z^\star)^\top & D\left(g(x^\star)\right) & 0 \\ A(z^\star)^\top & 0 & 0 \end{bmatrix}^{-1} \begin{bmatrix} -\left(\frac{\partial \mathcal{L}}{\partial z^\star}\right)^\top \\ 0 \\ 0 \end{bmatrix}}_{\text{BPQP solution: } [\tilde{z}, \tilde{\lambda}, \tilde{\nu}]^\top}. \tag{29}$$

7.3 Preserve KKT Norm Gradients

In a typical optimization algorithm, each stage of the iteration gives primal-dual conditions $r^{(k)}$, we follow the procedures of BPQP and solve the corresponding QP problem $\mathcal{Q}^{(k)}$ to define general gradients $\nabla_y \mathcal{L}^{(k)}$. The key difference here is that instead of using the optimal solution to derive BPQP, we plug in the intermediate points. By IFT,

$$dr^{(k)} = K^{(k)}[dz, d\lambda, d\nu]^\top + \frac{\partial r^{(k)}}{\partial y} dy = 0. \tag{30}$$

where $K^{(k)}$ is the Hessian matrix (KKT matrix) at points (z_k, λ_k, ν_k). The general gradients $\nabla_y \mathcal{L}^{(k)}$ is given by $dr^{(k)} = 0$ and therefore $\|r^{(k)}\| = C_k$ preserves KKT norm.

7.4 Simulation Experiment

Compared Methods

In Section 5.1, we randomly generate simulated constrained optimization datasets with uniform distributions and varying scales. We use these datasets to evaluate the efficiency and accuracy of state-of-the-art differentiable convex optimizers as well as BPQP. The methods of comparison briefly introduced previously are now detailed below:

- **CVXPY** is a universal differentiable convex solver [17, 6, 7]. SCS [32, 33] solver is employed to accelerate the gradients calculation process.
- **qpth/OptNet**: qpth is a GPU-based differentiable optimizer, OptNet [8] is a differentiable neural network layer that wraps qpth as the internal optimizer.
- **BPQP** is our proposed method. Its forward and backward passes are implemented in a decoupled way. It adopts the OSQP [12] as the forward pass solver. In the backward pass, it reformulates the backward pass as an equivalent simplified equality-constrained QP. OSQP is also adopted in the backward pass to solve the QP.
- **Exact** uses the same forward pass solver as BPQP. The optimization algorithm used for the forward pass is the OSQP [12], which is a first-order optimization algorithm that does not share differential structure information. In the backward pass, without using reformulation via BPQP, the Eq. (9) are solved using the matrix inversion method. As a result, this approach fails to achieve overall efficiency.

Hardware Setting

All results were obtained on an unloaded 16-core Intel(R) Xeon(R) CPU E5-2630 v3 @ 2.40GHz. qpth runs on an NVIDIA GeForce GTX TITAN X.

7.5 Portfolio Optimization Experiment

Statistical Risk Model (SRM)

SRM is used to generate the covariance matrix of MVO in Section 5.2. It takes the first 10 components with the largest eigenvalues by applying PCA on stock returns in the last 240 trading days. SRM shows the best performance of the traditional data-driven approach for learning latent risk factors.

Dataset & Metrics

This section provides a more detailed introduction to the datasets and metrics used in the experiments described in Section 5.2. The dataset is from Qlib [34] and consists of 158 sequences, each containing OHLC-based time-series technical features [35] from 2008 to 2020 in daily frequency. Our experiment is conducted on CSI 500 universe which contains at most 500 different stocks each day.

For the predictive metrics, we evaluate IC (Information Coefficient) and ICIR (IC Information Ratio) of predictive model baselines. IC measures the correlation coefficient between the predicted stock returns $\hat{y}$ and the ground truth y. At each timestamp t, $IC^{(t)} = corr(\hat{y}^{(t)}, y^{(t)})$ in which

$$corr(\mathbf{x}, \mathbf{y}) = \frac{\sum_i (x_i - \bar{x})(y_i - \bar{y})}{\sqrt{\sum_i (x_i - \bar{x})^2 \sum_i (y_i - \bar{y})^2}}.$$

We report average IC across instances. $ICIR = \frac{mean(IC)}{std(IC)}$ measures both the average and stability of IC. A well-trained predictive model is expected to have higher IC and ICIR. For portfolio metrics, which measure the performance of investment strategies in the real market, we include two key indicators, $Ann.Ret.$ (Annualized Return) and $Sharpe$ (Sharpe Ratio) , which are the ultimate criterion widely used in quantitative investment. $Ann.Ret.$ indicates the return of given portfolios each year. $Sharpe = \frac{Ann.Ret.}{Ann.Vol.}$ in which $Ann.Vol.$ indicates the annualized volatility. To achieve higher $Sharpe$, portfolios are expected to maximize the total return and minimize the volatility of the daily returns. Transaction cost is not considered in our portfolio metrics to align with the regret loss and more stably demonstrate the effectiveness of end-to-end learning without being distracted by unconsidered random factors.

Compared Methods

Here is a more detailed explanation of the compared methods in this experiment.

- **Two-Stage** separately learns a prediction MLP model to predict expected returns (i.e. μ) and then generates decisions based on Eq. (24). All other methods below share the same prediction MLP model and only differ in the learning paradigm.
- **DC3** is a learning-to-optimize-based optimizer for hard constraints optimization [19] by adding a gradients correction procedure. It is an approximation approach with high efficiency and low accuracy. We train the solver net (i.e. optimizer) with 500 epochs, 10000 samples, and 10 correction Test Max Steps for each type of QP and LP entries.
- **BPQP** is our proposed method. All the accurate approaches (e.g. CVXPY, qpth/OptNet) have similar high-quality solutions in both forward and backward passes and are expected to have similar performance. Among them, only BPQP can handle the problem size of 500 variables(refer to Table 1), and thus BPQP are selected.

BPQP and DC3 are trained using the loss function described in Section 7.1. In predict-then-optimize, inaccurate gradients can significantly mislead the final decision optimization, as empirical regret is subject to severe fluctuations. This can result in a significant decision error for the low-accuracy DC3, as shown in Table 2. Low-accuracy gradients are noisy and less in conflict with predictions. Therefore, DC3's prediction performance is similar to that of Two-Stage and better than BPQP.

Experiment setting

Here are the detailed search space for model architecture and hyper- parameters:

-